E. Tuovinen, J. Härkönen, P. Luukka, E. Tuominen, E. Verbitskaya, V. Eremin, I. Ilyashenko, A. Pirojenko, I. Riihimäki, A. Virtanen, and K. Leinonen, Czochralski silicon detectors irradiated with 24 GeV/*c* and 10 MeV protons, Nuclear Instruments and Methods in Physics Research A 568 (2006) 83-88.

Available online at www.sciencedirect.com
ScienceDirect
Nuclear Instruments and Methods in Physics Research A 568 (2006) 83–88
NUCLEAR INSTRUMENTS & METHODS IN PHYSICS RESEARCH Section A
www.elsevier.com/locate/nima

Czochralski silicon detectors irradiated with 24 GeV/c and 10 MeV protons

E. Tuovinen[a,*], J. Härkönen[a], P. Luukka[a], E. Tuominen[a], E. Verbitskaya[b], V. Eremin[b], I. Ilyashenko[b], A. Pirojenko[c], I. Riihimäki[c], A. Virtanen[c], K. Leinonen[d]

[a]*Helsinki Institute of Physics, P.O. Box 64, 00014 Helsinki University, Finland*
[b]*Ioffe Physico-Technical Institute of Russian Academy of Sciences, St. Petersburg, Russia*
[c]*Accelerator Laboratory, Jyväskylä University, Finland*
[d]*Lappeenranta University of Technology, Lappeenranta, Finland*

Available online 21 June 2006

Abstract

We have irradiated Czochralski silicon (Cz-Si) and Float Zone silicon (Fz-Si) detectors with 24 GeV/c and 10 MeV protons. Samples were characterized with Capacitance-Voltage measurements (CV), Transient Current Technique (TCT) and secondary electron backscattering recorded by Scanning Electron Microscope (SEM). We present the evolution of the effective doping concentration as a function of irradiation fluence as well as the introduction rate of negative space charge, β-parameter. According to these measurements, we found that Cz-Si is more radiation hard than Fz-Si. Both TCT and SEM measurements indicated that Space Charge Sign Inversion (SCSI) occurred in the heavily irradiated Fz-Si and in the Cz-Si irradiated with 10 MeV protons. However, the SCSI did not take place in Cz-Si irradiated with 24 GeV/c protons even after high irradiation fluence.

PACS: 85.30

Keywords: Silicon detectors; Radiation hardness; Czochralski silicon; Transient current technique; Scanning electron microscope

1. Introduction

Silicon detectors in High-Energy Physics (HEP) experiments are exposed to very hostile radiation environment. A possible upgrade of the luminosity of the CERN LHC (Large Hadron Collider) up to $10^{35}\,cm^{-2}\,s^{-1}$ has recently been proposed. This would raise the fluencies of fast hadrons up to $10^{16}\,cm^{-2}$, well beyond the operational limits of present silicon detectors. Particle radiation causes irreversible crystallographic defects in the silicon material thus inducing generation-recombination centers that in turn result in an increased detector leakage current. Additionally, the defects compensate the initial space charge of the n-type silicon created by the donor doping [1] which leads to changes in depletion voltages.

The sensors used in particle tracking systems must be fully depleted at reasonably low operating voltages, typically less than 400 volts for a 300 μm thick detector. Therefore, silicon sensors have traditionally been fabricated on wafers made by Float Zone crystal growth technique [2]. Float Zone technique ensures the growth of high-purity and sufficiently defect-free silicon crystals that are basic requirements for producing high-resistivity silicon substrates for detector applications. On the other hand, Float Zone silicon (Fz-Si) has characteristically a low oxygen concentration because of a contact-less and crucible-free crystal growth technique. However, the low oxygen concentration in Fz-Si is a drawback since oxygen has experimentally been found to improve the radiation hardness of silicon detectors, as demonstrated by the R&D work performed in the framework of CERN-RD48 collaboration [3,4].

Czochralski crystal growth method enables the production of silicon wafers with sufficiently high resistivity and

*Corresponding author. Tel.: +358 9 451 2365; fax: +358 9 451 5008.
E-mail address: esa.tuovinen@helsinki.fi (E. Tuovinen).

0168-9002/$ - see front matter © 2006 Elsevier B.V. All rights reserved.
doi:10.1016/j.nima.2006.05.208

with well-controlled oxygen concentration [5]. Although the Czochralski silicon (Cz-Si) is the basic raw material for microelectronics industry, high resistivity ($>1\,k\Omega\,cm$) Cz-Si wafers suitable for detector fabrication have become available only recently. This is likely due to the lack of commercial applications where both high resistivity and tailored oxygen concentration would be required.

In addition to the potential radiation hardness, Cz-Si as detector material may offer some economical benefits. Cz-Si wafers are available up to the diameter of 300 mm, while Fz-Si wafers have typically the diameter of 100–150 mm. Thus, using Cz-Si, very large area silicon detectors could be manufactured which in turn could result in significant savings in the costs related to front-end electronics, interconnection and module assembly.

In this study, we processed pad detectors on Cz-Si and standard Fz-Si wafers. Later, we irradiated the detectors with 10 MeV and 24 GeV/c protons. The irradiation fluencies were from $5\times10^{13}\,cm^{-2}$ to $5\times10^{15}\,cm^{-2}$ expressed in 1 MeV neutron equivalent fluences. After irradiations, full depletion voltages were measured from the detectors. Additionally, we have studied the Space Charge Inversion (SCSI) in the detectors by Transient Current Technique (TCT) and Scanning Electron Microscope (SEM) measurements.

2. Sample processing

In this study, we used 100 mm n-type 300 μm thick Cz-Si wafers manufactured by Okmetic Ltd as the starting material. The resistivity of the wafers is about 1100 Ω cm. The wafers have a homogenous oxygen concentration of about 7 ppm (American Standard TM). Additionally, we used 100 mm n-type 280 μm thick Fz-Si wafers with the resistivity of 1200 Ω cm manufactured by Wacker.

Using a very simple five mask level process, we processed $p^+/n^-/n^+$ diodes at the Microelectronics Center of Helsinki University of Technology. The p^+-implanted area of the diodes is 5 mm × 5 mm. One 100 μm wide guard ring surrounds the active area of the diode. This wide guard ring is surrounded by a multi-guard ring structure of 16 rings, each with a width of 15 μm. The detailed device structure is presented in Ref. [6]. The processing is described more in detail in Ref. [7]. The full depletion voltage, extracted from Capacitance-Voltage (CV) measurements, is about 300 V for Cz-Si diodes and 260 V for Fz-Si diodes. The leakage current at full depletion was less than 5 nA for all diodes. Randomly selected diodes were measured above the full depletion voltage, up to 1000 V, without observing breakdown [8].

3. Irradiations

The irradiation with 10 MeV protons was carried out at Jyväskylä University Accelerator Laboratory. Diodes were first glued with photoresist to ceramic supports so that four diodes were always placed on each support. Samples were placed inside a vacuum chamber at the end of RADiation Effects Facility (RADEF) beam line [9]. The intensity of the proton beam was $\sim2\,nA/cm^2$. Samples were kept at −10 °C during the irradiation.

The irradiation with 24 GeV/c high-energy protons was performed at CERN Irrad1 facility operating by PS accelerator [10]. During the irradiation at about 27 °C the samples were not biased.

For the transformation of the proton fluence values for 10 MeV and 24 GeV/c to the equivalent values of 1 MeV neutron fluence, the hardness factors 4.32 and 0.6, respectively, were used as presented in Ref. [11]. After the irradiations, samples were stored at a temperature below −10 °C.

4. Capacitance-Voltage (CV) characteristics

Before the measurement, the diodes were annealed at 80 °C for 4 min. Prior to the irradiations, the variation of the full depletion voltage was in the order of 10% and 5% for the Fz-Si and Cz-Si diodes, respectively [12]. In our previous study, we have observed that in the case of 10 MeV protons the space charge sign inversion (SCSI) in the Cz-Si material of this resistivity takes place at about $2\times10^{14}\,cm^{-2}$ 1 MeV neutron equivalent fluence [13].

The full depletion voltages (V_{fd}) of the irradiated diodes were resolved from CV measurements. The effective doping concentration (N_{eff}) of the silicon material was calculated from the extracted V_{fd} values. The results of Cz-Si and Fz-Si samples are presented in Figs. 1 and 2, respectively. Each data point corresponds to an individual diode irradiated with a specific fluence. A curve was fitted to the data points in order to better visualize the evolution of the effective doping concentration N_{eff}. The values of N_{eff} for the Fz-Si diodes have been normalized to the thickness of 300 μm. As seen in Figs. 1 and 2, the effective doping concentration of

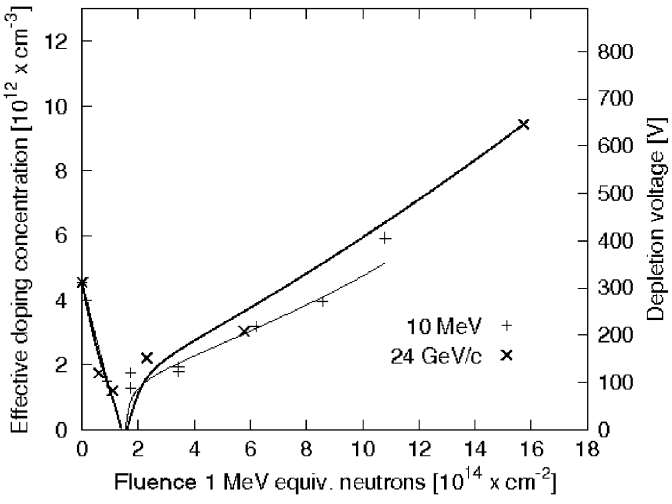

Fig. 1. The evolution of effective doping concentrations (N_{eff}) in Cz-Si pad detectors irradiated with 10 MeV (+) and 24 GeV/c (x) protons.

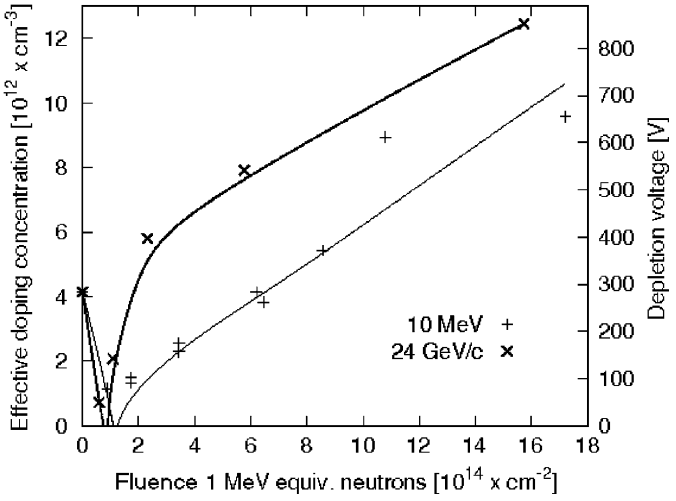

Fig. 2. The evolution of effective doping concentrations (N_{eff}) in Fz-Si pad detectors irradiated with 10 MeV (+) and 24 GeV/c (x) protons.

Cz-Si is less sensitive to the increased radiation fluence than that of Fz-Si.

As seen in Figs. 1 and 2, in the case of both Fz-Si and Cz-Si, a deviation from the general trend of N_{eff} is observed at the fluence value of about $10^{15}\,cm^{-2}$ 1 MeV neutron equivalent. This is probably due to the inaccuracy in the beam current measurement during the irradiation of the specific ceramic support holding these samples.

Furthermore, straight lines were fitted to the data points, presented in Figs. 1 and 2, after the minimum of the effective doping concentration, N_{eff}. The slope of this line, or the increase of N_{eff} beyond the minimum point, is called β-parameter. This is the introduction rate of negative space charge beyond the inversion point, resulting from the radiation induced deep acceptors.

The extracted values of the β-parameters for different materials and different proton irradiations are listed in Table 1. In general, low β-parameter indicates high radiation tolerance since the material changes less as a function of the radiation fluence.

As seen in Table 1, the β-parameter of the Cz-Si material irradiated with 24 GeV/c high-energy protons is about 30% higher than that of the Cz-Si material irradiated with 10 MeV low energy protons.

In the case of Fz-Si irradiated with low-energy 10 MeV protons, the β-parameter can easily be fitted since the data points show good linear behavior after the inversion point. However, in the case of Fz-Si irradiated with 24 GeV/c high-energy protons, the extraction of β-parameter is not straightforward because the Fz-Si diodes receive considerable damage before the saturation around the value of $2 \times 10^{14}\,cm^{-2}$ 1 MeV neutron equivalent fluence (see Fig. 2).

If we compare the values of the β-parameters of Fz-Si and Cz-Si taking into account the limitations for the case of Fz-Si discussed previously, we can consider that Cz-Si is more radiation tolerant than Fz-Si.

Table 1
β-parameters of different materials and irradiations

Irradiation	Material	
	Cz-Si	Fz-Si
10 MeV	0.0043	0.0058
24 GeV/c	0.0056	(0.0049)

5. TCT measurements and electric field analysis

One Fz-Si and one Cz-Si pad detector from both irradiations was selected for further investigation with Transient Current Technique (TCT). This method is based on the generation of non-equilibrium carriers by laser pulse [14].

The current pulse response of the detectors irradiated by 10 MeV protons with the 1 MeV equivalent fluence of $1.1 \times 10^{15}\,cm^{-2}$ showed double peak (DP) shape irrespective of the type of silicon. The detectors were measured from both p^+ and n^+ sides in a certain range of bias voltage. The DP in the TCT curve of an irradiated sample indicates that the SCSI has occurred.

As an example, the TCT curves of the Fz-Si detector #56 are presented in Fig. 3. The range of reverse bias was from 128 to 475 V. The enlarged tail in the current pulse disappears at 300 V indicating the full depletion of the detector. The DP shape is observed starting from 240 to 300 V for the signals from p^+ and n^+ side, respectively.

In addition, the Cz-Si detector irradiated by 10 MeV protons with the 1 MeV neutron equivalent fluence of $1.8 \times 10^{15}\,cm^{-2}$ showed similar DP performance. On the contrary, the current pulse response measured from the Cz-Si detector irradiated by 24 GeV/c protons with the 1 MeV neutron equivalent fluence of $1.8 \times 10^{15}\,cm^{-2}$ showed only a single peak indicating no SCSI. This was independent of the side (p^+ or n^+) that was illuminated.

A novel simulation and fitting program was used to analyze the transient current responses with DP shape. The fitting procedure is based on the new approach for characterization of heavily irradiated silicon detectors developed in Ref. [15]. This approach is based on a detector model that consists of three regions (see Fig. 4): 1 and 2 are space charge regions near the p^+ and n^+ contacts, respectively, and B is an electrically neutral base region. The effective space charge concentrations N_{eff1} and N_{eff2} near the p^+ and n^+ contacts, respectively, are assumed to be constant. Therefore, the electric field in the regions 1 and 2 has a linear distribution. The charge carriers generated by the laser pulse are trapped while they drift through the detector thickness. The trapping is defined by the trapping time constant τ, which is different for electrons and holes.

$$q = q_0 \exp(-t/\tau) \quad (1)$$

where q is a the moving charge, q_0 is the generated charge and t is time.

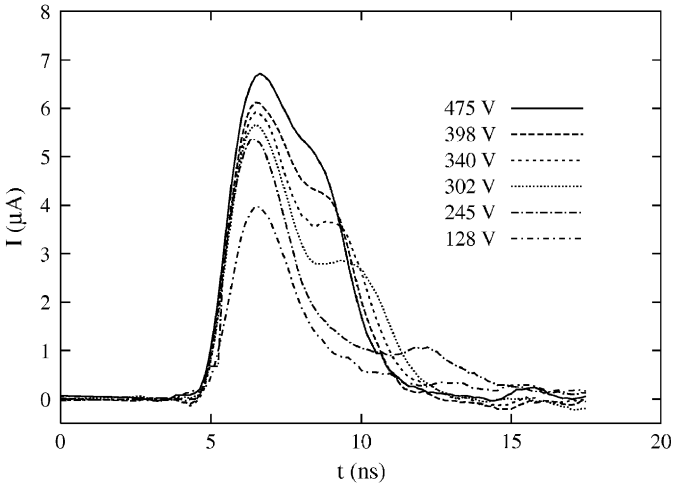

Fig. 3. The TCT curves obtained by illuminating the p^+ contact (front side) of the Fz-Si pad detector #56.

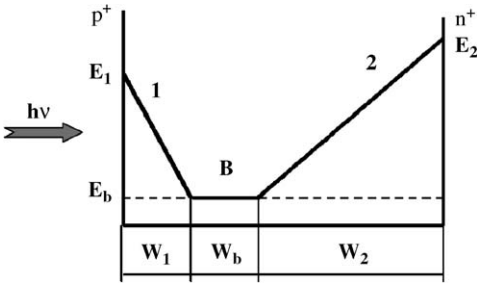

Fig. 4. Electric field distribution in a heavily irradiated Si detector assuming a non-zero electric field in the base region B.

The new aspect in the modeling of the TCT signal and in the reconstruction of the electric field profile $E(x)$ developed in Ref. [15] is the rise of the significantly high electric field E_b in the neutral base region of the heavily irradiated detectors. The electric field originates from the current flow through the detector and from the consequent drop of the potential across the high resistivity bulk of the non-depleted region. This electric field stimulates the drift of the collected carriers through the base region. The response of the induced current pulse can be simulated as a result of the carrier drift through the entire thickness of the detector. In other words, this approach allows the electric field reconstruction from the detector current pulse response.

As an example, Fig. 5 presents the experimental pulse response measured from the p^+ side of the Fz-Si detector #56 operated at $V = 398\,\mathrm{V}$ as well as the simulated response. As seen in the graph, the two curves are quite compatible. The corresponding $E(x)$, reconstructed from the pulse response, is shown in Fig. 6.

The parameters of the $E(x)$ distribution were extracted from the fit and are presented in Table 2. The trapping time constant for electrons τ_e is 2.3 ns that agree with data for heavily irradiated silicon detectors reported in Ref. [6]. Using the parameter values defined from the fit of the pulse response from the p^+ side, we made a fit of the signal from the detector n^+ side by adjusting mainly one parameter, namely the trapping time constant for holes, τ_h. The results are presented in Table 2.

According to the results presented in Fig. 6 and Table 2, the $E(x)$ is non-uniform and the corresponding concentra-

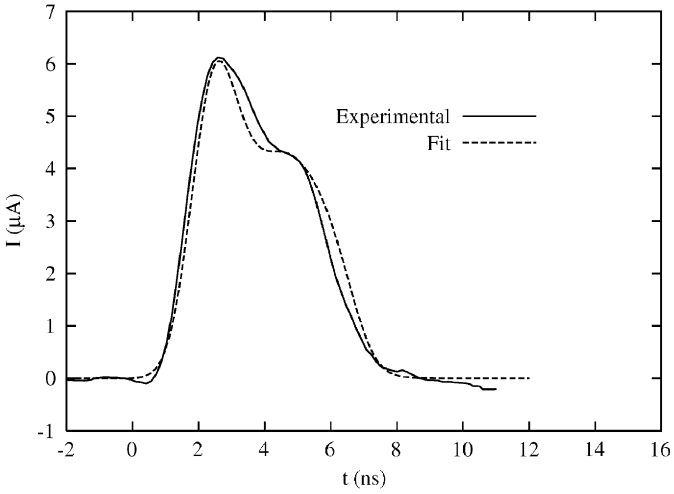

Fig. 5. The experimental pulse response from the p^+ side of the Fz-Si pad detector #56 operated at $V = 398\,\mathrm{V}$ and the simulated response.

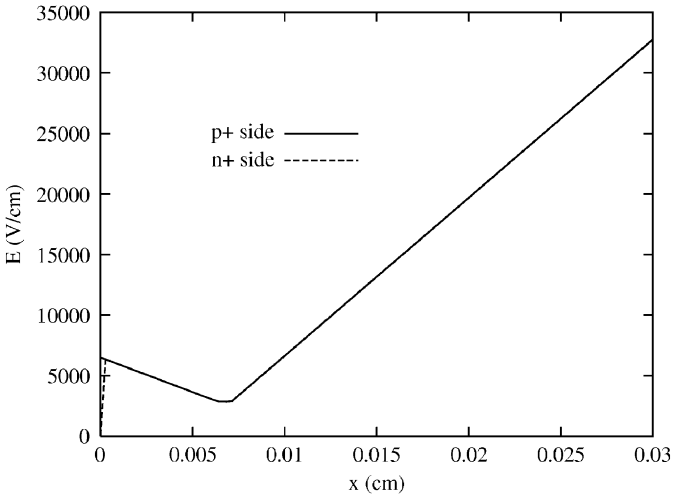

Fig. 6. Electric field distribution reconstructed from the pulse response presented in Fig. 5.

Table 2
Parameters extracted from the fit of the current pulse response of detector #56 processed on Fz-Si and operated at $V = 398\,\mathrm{V}$

	p^+ side	n^+ side
τ_e (ns)	2.3	
τ_h (ns)		1.3
N_{eff1} (cm^{-3})	8.2×10^{11}	8.4×10^{11}
N_{eff2} (cm^{-3})	-7.8×10^{12}	-7.8×10^{12}
E_b (kV/cm)	2.8	2.8
W_b (μm)	7	7

tions N_{eff1} and N_{eff2} near the p^+ and n^+ contacts, respectively, differ by a factor of 10 and have different signs. The trapping time constants are in the range of few nanoseconds. Since the trapping time constant is inversely proportional to the fluence [16], the amount of free carriers trapped in the region 1 increase with the increasing fluence resulting in a significant reduction of the second peak in the shape of DP response until it is totally disappeared.

We continue to study the electric field reconstruction in the bulk of the heavily irradiated detectors processed on different types of silicon. The results in the reconstruction of $E(x)$ obtained earlier in Ref. [15] showed that the parameters of the electric field profile are sensitive to the detector processing.

6. SEM measurements

The diodes characterized by TCT were prepared for SEM studies. All sample chips were cut into two halves (along the ⟨100⟩ crystal plane) with an ordinary diamond pen and bending method in order to get as clean and unscratched surface as possible. The quality of the samples after the cleaving was checked by IV and CV measurements. As expected, after the cutting the absolute value of capacitance decreased by factor of about two. The leakage current remained essentially unchanged, i.e. the leakage current density approximately doubled due to the sample cleaving.

The cleaved detector is placed in the vacuum chamber of the scanning electron microscope into an upright position. The bias voltage was fed over the detector from an Agilent semiconductor parameter analyzer, VSMU and its associated voltage (V) and current (A) meters constituting one SMU (Source Measure Unit). A 5 keV electron beam scanned over the cross-section of the cleaved detector from the p^+ contact to the n^+ contact at a speed of 2–5 μm/s.

The primary 5 keV electron beam generates secondary electrons at most a few nanometers below the examined surface. These electrons were pulled to a secondary electron detector (SEI = Secondary Electron Image) by a positive voltage VSEI around this detector. The value of VSEI is fixed to 10 kV in this microscope. The secondary electron signal is amplified and converted digital in a 12-bit ADC. This signal plus the horizontal and vertical timing signals of the scanning electron microscope are read to a PC using C++ software.

The energy of secondary electrons is small, less than 50 eV. So even a small positive voltage on the sample can decrease the number of electrons arriving to the secondary electron detector and hence cause a phenomenon called voltage contrast. This has been utilized in the current work. The contrast, C, is converted to voltage, V, according to equation:

$$V = -M \ln(1 + C/K), \quad (2)$$

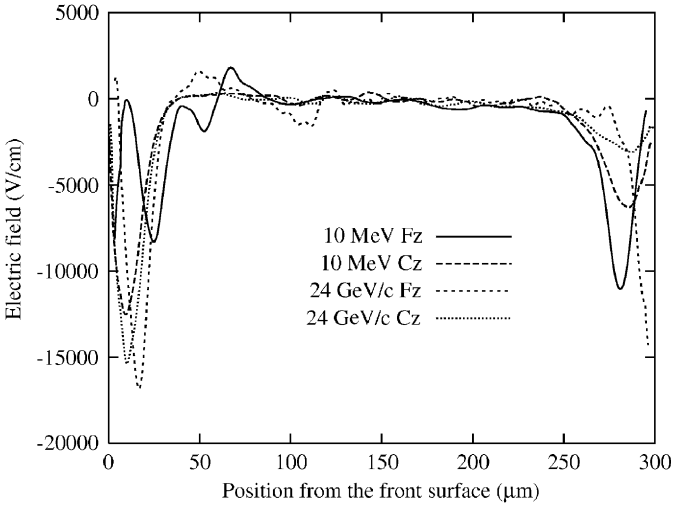

Fig. 7. Electric field distribution in silicon bulk acquired by SEM measurement. The detectors are biased with 40 V. The p+ contact is on the left and the n+ contact is on the right.

where the contrast scaling factor K and the voltage constant M are found by the procedure described in Refs. [17,18].

A drawback of this method is that with our measurement setup the voltage contrast starts to saturate at relative small voltages. With this method, it is therefore impossible to characterize heavily irradiated detectors under full depletion conditions. With 40–60 V bias we are, however, able to see clear, non-saturated, voltage contrast. This is sufficient to see from which side of the detector the electric field starts to extend.

Electric field distribution in Fig. 7 was extracted from the voltage contrast data. DP of the electric field can be seen in all samples except in the 24 GeV/c Cz-Si pad detector.

7. Conclusions

Defects can roughly be divided into two categories: point defects (mainly vacancies and their complexes) and defect clusters. Generally, low-energy protons (e.g. 10 MeV) cause mainly point defects meanwhile high-energy protons (e.g. >50 MeV) induce dominantly clustered defect complexes into the silicon lattice. Additionally, the interaction of oxygen atoms with defects, or in other words the beneficial effect of oxygenation, is dependent on the energy of the incident proton irradiation. Defect formation mechanism are discussed more in detail e.g. in Refs. [19,20].

The energy dependence of the β-parameter can be attributed to the different defect formation kinetics. In our study, the β-parameters extracted from the evolution of effective doping concentration indicate better radiation hardness for Cz-Si than for float zone silicon.

The electric field in heavily irradiated samples was studied by TCT and by secondary electron backscattering recorded by SEM. These two measurement methods are fundamentally different. SEM method is a steady state measurement and is not influenced by trapping. On the

Table 3
TCT and SEM measurement results

Sample	Proton energy	Proton fluence p/cm^2	DP TCT	DP SEM
FZ #34	24 GeV/c	3.0×10^{15}	X	X
FZ #56	10 MeV	2.5×10^{14}	X	X
CZ #29	24 GeV/c	3.0×10^{15}		
CZ #36	10 MeV	2.5×10^{14}	X	X

other hand, trapping influences current transient measurements that are commonly adopted among the scientific community of radiation hardness studies.

In this study, the double peak (DP) of the electric field was found by both measurements in all the Fz-Si samples and in the 10 MeV proton irradiated Cz-Si sample. However, the double peak was not observed in the 24 GeV/c proton irradiated Cz-Si sample indicating that the space charge sign inversion has not occurred. The results are summarized in Table 3.

The electric field profile is the key parameter responsible for the charge collection efficiency in silicon detectors. Therefore, in future we will further study the electric field distribution in heavily irradiated silicon detectors.

The 300 μm thick Cz-Si detectors were fully depleted at about 600 V after the 1 MeV neutron equivalent fluence of 2×10^{15} cm^{-2}. This fluence corresponds roughly the radiation environment in the innermost pixel detector layers during the full lifetime of LHC experiments [21]. Replacement of the Fz-Si tracking pixel detectors, placed in the most harsh radiation environment, is scheduled to take place during the operation of the experiments.

The 300 μm thick detectors subjected to the fluence of 1×10^{16} p/cm^{-2} of 24 GeV/c protons could not be depleted below the voltage of 1000 V. The extrapolation of the capacitance-voltage data suggests that these detectors would be depleted at about 2 kV corresponding of N_{eff} of about 2.9×10^{13} cm^{-3}. However, pixel detectors are commonly processed on 200 μm thick silicon substrates. Thus, a Cz-Si device with corresponding N_{eff} would be depleted at about 800 V. Therefore, the Cz-Si material with high oxygen concentration could be an interesting alternative for upgrades of tracking systems in LHC experiments.

Acknowledgments

Authors are most grateful to Dr. Michael Moll, Dr. Maurice Glaser and Federico Ravotti from CERN for providing the 24 GeV/c irradiations and for their assistance in the CV and IV measurements. This work has been performed within framework of CERN RD39 and RD50 collaborations. This work was partially financed by the Academy of Finland.

References

[1] G. Lindstrom, et al., Nucl. Instr. and Meth. A 426 (1999) 87.
[2] G. Lutz, Semiconductor Radiation Detectors, Device Physics, Springer, Berlin, 2001, p. 260.
[3] G. Lindström, et al., Nucl. Instr. and Meth. A 466 (2001) 308.
[4] A. Ruzin, et al., IEEE Trans. Nucl. Sci. NS-46 (5) (1999) 1310.
[5] V. Savolainen, et al., J. Cryst. Growth 243 (2) (2002) 243.
[6] RD50 Status Report, CERN/LHCC-2003-058 (2003) 30.
[7] J. Härkönen, et al., Nucl. Instr. and Meth. A 514 (2003) 173.
[8] E. Tuovinen, Processing of Cz-Si Pad Detectors with Different Thermal Treatments, Third RD50 Workshop on Radiation Hard Semiconductor Devices for Very High Luminosity Colliders, CERN, November 3–5, 2003.
[9] A. Virtanen, et al., Nucl. Instr. and Meth. A 426 (1999) 68.
[10] ⟨http://irradiation.web.cern.ch/irradiation/irrad1.htm⟩.
[11] A. Vasilescu (INPE Bucharest), G. Lindstroem, Displacement Damage in Silicon, University of Hamburg, on-line compilation, ⟨http://sesam.desy.de/members/gunnar/Si-dfuncs.html⟩.
[12] J. Härkönen, et al., Nuclear Science Symposium Conference Record, vol. 3, IEEE, New York, 16–22 October 2004, pp. 1999–2002.
[13] E. Tuominen, et al., IEEE Trans. Nucl. Sci. NS-50 (2003) 1942.
[14] V. Eremin, et al., Nucl. Instr. and Meth. A 372 (1996) 188.
[15] E. Verbitskaya, et al., Nucl. Instr. and Meth. A 557 (2006) 528.
[16] V. Eremin, Nucl. Instr. and Meth. A 372 (1996) 388.
[17] K. Leinonen, et al., Nucl. Instr. and Meth. A 552 (2005) 357.
[18] K. Leinonen, Nucl. Instr. and Meth. A 555 (2005) 411.
[19] M. Huhtinen, Nucl. Instr. and Meth. A 491 (2002) 194.
[20] I. Pintilie, et al., Nucl. Instr. and Meth. A 514 (2003) 18.
[21] CMS Technical proposal, CERN/LHCC 94-38, 1994.